

# Preparation and *in vitro* evaluation of Vancomycin loaded Montmorillonite-Sodium Alginate topical gel for wound infection

Ladan Dayani<sup>1</sup>, Azade Taheri<sup>1\*</sup>, Somayeh Taymouri<sup>1</sup>,  
Rahim Bahri Najafi<sup>1</sup>, Fereshteh Esmailian<sup>1</sup>

<sup>1</sup>Novel Drug Delivery Systems Research Center, Department of Pharmaceutics,  
Faculty of Pharmacy, Isfahan University of Medical Sciences, Isfahan, Iran

Despite decades of research, wound healing remains a significant public health problem. This study aimed to develop and evaluate a topical sodium alginate gel containing vancomycin (Van) loaded MMT NPs for wound healing applications. Van was loaded in MMT at different conditions (pHs of 6, 7 and temperatures of 40, 50 °C) (Van/MMT NPs). The optimum formulation (with the smallest particle size and a high value of zeta potential;  $270.8 \pm 77.35$  nm and  $-35.96 \pm 2.73$ , respectively) showed a high drug-loading capacity (entrapment efficacy of 96%) and a sustained release pattern of Van (95%) over 480 min. The optimum Van/MMT NPs were embedded into the sodium alginate (SA) gel (Van/MMT NPs/SA gel). The Van/MMT NPs/SA gel showed a sustained and slow release pattern of Van (95%) over 50 h. FTIR tests revealed the electrostatic interaction between MMT and Van. The broth macrodilution tube method was used to determine the minimum inhibitory concentration (MIC) of Van, Van/MMT NPs, and Van/MMT NPs/SA gel against *Staphylococcus aureus*. The results showed the promising antibacterial activity of Van/MMT NPs/SA gel, thus, this gel can be a promising formulation for the management of infected wounds.

**Keywords:** Montmorillonite. Sodium alginate. Vancomycin. Wound healing, Antibacterial effect. Gel.

## INTRODUCTION

Acute and chronic non-healing wounds are found as one of the most important health issues that have a significant financial burden on health care systems all over the world (Han, Ceilley, 2017). Chronic non-healing wounds are classified as those that have a poorly healing manner and persist for at least 3 months (Stacey, 2018). Venous leg ulcers, arterial ulcers, diabetic foot ulcers, and pressure ulcers are examples of chronic non-healing wounds. However, acute wounds, including traumatic and surgical wounds, occur suddenly. These types of

wounds heal typically at a predictable and expected rate based on the normal wound healing process (Krzyszczuk *et al.*, 2018).

Skin lesions have been indicated to be easily infected with bacteria, resulting in delayed wound healing and increased pain (Masson *et al.*, 2017; Menke *et al.*, 2007). Surgical-site infection, the most common form of hospital-acquired infections, seems to occur due to delayed wound healing, or prolonged hospital stays (Schweizer *et al.*, 2015). Despite decades of research, treatment of infected wounds remains one of the most important challenges. Systemic antibiotic therapy has been previously used as a usual intervention, however, later attempts have been included in local wound management such as using wound dressings containing antiseptics or antibiotics (Hey *et al.*, 2017). The main aim of antiseptics or antibiotic-containing

\*Correspondence: A. Taheri. Novel Drug Delivery Systems Research Center. Department of Pharmaceutics. Faculty of Pharmacy. Isfahan University of Medical Sciences. Isfahan, Iran. Fax: 0098 3136692288. E-mail: az.taheri@pharm.mui.ac.ir. ORCID: <https://orcid.org/0000-0002-2256-040X>. Ladan Dayani –ORCID: <https://orcid.org/0000-0001-9931-4664>. Somayeh Taymouri – ORCID: <https://orcid.org/0000-0001-6089-8367>

wound dressings is to achieve a healed closed wound, enhance the wound healing rate, and protect the wound from infection (Gonzalez *et al.*, 2016).

In addition to local delivery of antibiotics that decreases their systemic side effects, the sustained delivery of antibiotics at the wound site can also protect the wound from re-infection and re-contamination, reduce the frequency of dressing changes, provide better antibacterial activity, and improve tissue regeneration simultaneously (Kurczewska *et al.*, 2015; Li *et al.*, 2010; Zhang *et al.*, 2017). Nowadays, different wound dressings have been produced for the local sustained delivery of antibiotics at the wound site.

Vancomycin (Van) is a glycopeptide antibiotic that has the potential to eradicate the gram-positive bacterial infections such as methicillin-resistant *S. aureus* (MRSA), which is the typical infection found in wounds. Because of the high water solubility of Van, the preparation of a sustained release drug delivery system of Van is difficult. Many recent studies have attempted to prepare a sustained release system of Van for application in wound healing (Li *et al.*, 2010; Kim, Knowles, Kim, 2005) the clinical standard of care for treating contaminated open fractures comprises a staged approach, wherein the wound is first treated with non-biodegradable antibiotic-laden poly(methyl methacrylate). For example, a biodegradable porous polyurethane (PUR) scaffold of Van was employed by Li *et al.* (2010) for inhibiting the infection of bone wounds. Their formulation showed an 8-week sustained release pattern of Van. In another study, a scaffold of porous hydroxyapatite (HA) coated with a Van-containing poly( $\epsilon$ -caprolactone) (PCL) polymer was prepared as a wound dressing. The authors reported that 84.4% of Van was released from the prepared wound dressing after 72 h (Kim, Knowles, Kim, 2005).

Montmorillonite (MMT) is a hydrated aluminum silicate with a two-dimensional lamellar structure with Si–O tetrahedrons and Al–O(OH)<sub>2</sub> octahedrons on the bottom and top of the layers, respectively. Defects in the tetrahedral and octahedral sheets produce a negative charge for MMT, which is counterbalanced by sodium ions. Electron microscope analyses indicate that MMT particles are plate-shaped with an average diameter of 1  $\mu\text{m}$  and a thickness of 0.96 nm (Norrish,

1954; Meng *et al.*, 2009; Dening *et al.*, 2016). MMT is one of the most widely used phyllosilicate clay that has a large cation exchange capacity and excellent-nontoxic adsorbent properties because of its high aspect ratio. Some MMT characteristics, such as the ability of electrostatic interaction with positively charged drugs, loading of drug molecules between its layers, and controlled release of drug molecules, make it act as an effective carrier for sustained delivery of therapeutic agents (Joshi *et al.*, 2009; Salcedo *et al.*, 2012). MMT has been employed as a carrier to prepare stabilized nanoparticles (NPs) for the controlled release of drug delivery systems of metformin, valsartan, fenofibrate, dalcetrapib, and mefenamic acid (Feng *et al.*, 2009; Sandri *et al.*, 2014; Kumar *et al.*, 2020; Rebitski *et al.*, 2018) fungi and some viruses. However, AgSD has been shown to be cytotoxic toward fibroblasts and keratinocytes in vitro and consequently to retard wound healing in vivo. The aim of the present work was to evaluate the in vitro biocompatibility (cytotoxicity and proliferation).

Sodium alginate (SA) is a natural linear polysaccharide based on a biopolymer extracted from brown sea algae. The molecular structure of SA indicates that it consists of D-mannuronic and L-glucuronic acids, which are arranged to make a biocompatible, mucoadhesive, nontoxic, and inexpensive bipolymer. Due to its molecular structure, SA can form a gel in the presence of multivalent ions that could be used as an excellent vehicle for controlled drug delivery (Tønnesen, Karlsen, 2002). The placement of drug-loaded MMT into biopolymer-based gels or composites can improve the sustained release pattern of drugs from MMT (Wang, Du, Luo, 2008; Dong, Feng, 2005; Feng *et al.*, 2009; Wu, Li, Hong, 2013).

The current study aimed to investigate the release pattern and antimicrobial effect of Van-loaded montmorillonite NPs in the SA gel (Van/MMT NPs/SA gel) for the future development of effective hydrocolloid wound dressings. If Van/MMT NPs/SA gel shows a promising antimicrobial effect and a suitable sustained release pattern of Van, this gel will be freeze-dried and used as a novel hydrocolloid layer on a semipermeable film in a hydrocolloid wound dressing in our future study.

## MATERIAL AND METHODS

### Material

Montmorillonite (MMT) and vancomycin powder (Van) were purchased from Sigma Company. Sodium alginate (SA) was obtained from Merck Chemical Company (Germany). Deionized water was used throughout the experiment. All other chemicals used were of analytical reagent grades.

### Preparation of vancomycin nanoparticles (Van/MMT NPs)

To prepare the NPs, 120 mg of the MMT clay was dispersed in water (5 ml) and kept magnetically stirred in a water bath at 80 °C for 20 h. This procedure is useful to achieve a better yield of Van loading in the clay. Then, the dispersion was cooled to reach 40 °C. After that, 80 mg of Van was added to the mixture, the samples were kept magnetically stirred in a water bath at 40 °C for 10 min to obtain a homogeneous dispersion and then stirred on a magnetic stirrer (IKA-WERKE, Model RT 10 power, Japan) at 300 rpm for 4 h in different pHs (6 and 7) and temperatures (40 and 50 °C).

### Characterization of Van/MMT NPs

#### Particle size and Zeta potential analysis

The particle size, size distribution, and zeta potential of prepared the Van/MMT NPs in each formulation were measured using a Zetasizer (Zetasizer 3600, Malvern Instrument Ltd., Worcestershire, UK). Measurements were performed in triplicate.

#### Entrapment efficiency and loading efficiency

To obtain the entrapment efficiency of Van in the MMT NPs (Van/MMT NP), 5 ml of each mixture containing Van/MMT NPs was centrifuged at 7,000 rpm for 15 min. The amount of Van that loaded in the MMT nanoparticles was indirectly determined by

measuring the drug content in the supernatant. To do this, the supernatant was passed through a 0.45 µm filter membrane to remove the solid residues of MMT, and Van was quantified spectrophotometrically (UV-mini 1240, Shimadzu, Kyoto, Japan) at 280 nm after suitable dilution. Appropriate blank and calibration curves were used to calculate the accurate amount of loaded Van in NPs. The encapsulation efficiency (EE) and loading efficiency (LE) of Van in NPs were determined according to the following equations:

$$EE(\%) = \frac{\text{analyzed weight of entrapped drug}}{\text{theoretical weight of drug loaded in the system}} \times 100 \quad \text{eq 1}$$

eq 1

$$LE(\%) = \frac{\text{entrapped drug in dispersion}}{\text{total amount of polymer and drug}} \times 100 \quad \text{eq 2}$$

eq 2

All the measurements were done in triplicate.

#### Release of Van from Van/MMT NPs

To evaluate the release of Van from Van/MMT NPs, 2 ml of the prepared mixture containing Van/MMT NPs was placed into a dialysis bag (cutoff 12,000 Da) and placed into 18 mL of deionized water, which was constantly rotated on a magnetic stirrer at 400 rpm at 37 °C. At predetermined time intervals, 1 ml of the release medium was withdrawn, and the same volume was replaced by a fresh medium. Van was quantified in the release medium spectrophotometrically at 280 nm (UV-mini 1240, Shimadzu, Kyoto, Japan). Moreover, the dissolution efficiency (DE) up to 360 min was determined using the following equation:

$$DE_T = \frac{\int_0^T y_t \cdot dt}{y_{100} \cdot T} \quad \text{eq 3}$$

Mean dissolution time, which shows the mean time for the drug to dissolve under *in vitro* dissolution conditions, was also calculated using the following equation:

$$MDT = \frac{\sum_{j=1}^n t_j \Delta M_j}{\sum_{j=1}^n \Delta M_j} \quad \text{eq 4}$$

where  $j$  is the sample number,  $t_j$  is the midpoint of the  $j^{\text{th}}$  time period (easily calculated with  $((t+t_{i-1})/2)$ , and  $M_j$  is the additional amount of drug dissolved between  $t_j$  and  $t_{i-1}$ .

### Preparation and characterization of SA gel containing Van/MMT NPs (Van/MMT NPs/SA) gel

The Van/MMT NPs were added to the SA solution (8% w/v) under vigorous stirring (400 rpm). The resultant mixture was stirred at 40 °C to form a homogenous SA gel containing Van/MMT NPs (Van/MMT NPs/SA gel). The final concentration of Van in gels was 5 mg/ml. In this study, the SA gel containing blank MMT NPs (MMT NPs/SA gel) was used as a control.

#### *In vitro* release of Van from Van/MMT NPs/SA gel

The *in vitro* release test was performed using the Franz cell. A cellulose acetate membrane was located on the Franz cell receiver, and 1 ml of the SA gel containing Van/MMT NPs/SA gel was placed uniformly on the membrane in the donor enclosure. The Franz cell receiver was filled with 27 ml of the phosphate-buffered saline (PBS) medium (pH 7.4, 32 °C) while stirring at 400 rpm to mimic the human skin condition (Gelker *et al.*, 2018). At definite time intervals, 1 ml of the release medium was withdrawn and replaced with fresh PBS. The absorption of the samples was measured by spectrophotometric quantitative determination (UV-mini 1240, Shimadzu, Kyoto, Japan) at 280 nm. The Lambert–Beer law was used to determine the amount of released Van. The *in vitro* test was carried out in triplicate. To determine the release mechanism, the results of the *in vitro* release experiment were fitted to zero-order, first-order, Higuchi, Korsmeyer-Peppas, and Hixson-Crowell equations.

#### Fourier-transform infrared spectroscopy analysis (FTIR)

The FTIR analysis can demonstrate the potential physical or chemical interaction between the polymer and the drug. The FTIR spectra of pure MMT, pure Van, sodium alginate, physical mixture of Van and MMT, Van/MMT NPs, and freeze-dried Van/MMT NPs/SA gel were obtained using an FTIR spectroscope (Jasco, FTIR model 6300, Japan). Samples were prepared into potassium bromide pressed discs and scanned at a range of 4000–400  $\text{cm}^{-1}$  with 1.0  $\text{cm}^{-1}$  resolution.

#### Morphological characterization using scanning electron microscopy (SEM)

SEM micrographs of MMT, Van/MMT NPs, and Van/MMT NPs/SA gel were obtained using a SEM microscope (Hitachi F41100, Japan). To prepare the samples, they were mounted on an aluminum stub by a conductive double-sided adhesive tape, and then the coating procedure was conducted in an argon atmosphere with gold (Hitachi IonSputter, E-1030).

#### Microbial study

##### *Determination of the inhibition zone of Van/MMT NPs/SA gel against the pathogen*

The “well diffusion test” was carried out to determine the inhibition zones of Van, MMT/SA gel, Van/MMT NPs, and Van/MMT NPs/SA gel against *S. aureus* (ATTC 25923, gram-positive bacterium). The bacterial suspension with a cell density of 0.5 McFarland ( $1.5 \times 10^8$  CFU/mL) was transferred onto the surface of Muller–Hinton agar plates using sterile cotton swabs. Wells with 8 mm diameter were made in the agar plates using a sterile Pasteur pipette and filled with 80  $\mu\text{l}$  of each sample. Due to the high viscosity of the MMT/SA gel and Van/MMT NPs/SA gel, all the formulations contained SA diluted by 10 folds. The zones of inhibition around the wells were measured using a caliper after 72 h of incubation (37 °C, 5%  $\text{CO}_2$ ).

### Determination of minimum inhibitory concentration of Van/MMT NPs/SA gel against the pathogen

The minimum inhibition concentration (MIC) of Van, MMT, Van/MMT NPs, MMT/SA gel, and Van/MMT NPs/SA gel against *S. aureus* as gram-positive pathogenic bacteria was determined using the conventional broth macrodilution tube method.

A stock solution of Van (200 µg/ml) was prepared in sterile water, which was further diluted in Muller–Hinton broth to reach a concentration range of 0.5-10 µg/ml. For Van/MMT NPs, the MIC value was determined by geometric dilutions at final equal Van concentrations of 0.7, 1.4, 2.1, 2.8, 3.15, 3.5, 4.2, 4.9, 5.6, and 6.3 µg/ml. Concentrations of 1, 2, 3, 4, 4.5, 5, 6, 7, 8, and 9 µg/ml for MMT were also prepared as the blank. This procedure with the same concentrations was also used for MMT NPs/SA gel and Van/MMT NPs/SA gel. The bacterial concentration of each tube was adjusted to about  $5 \times 10^6$  CFU/ml. The negative control tube contained the culture medium without *S. aureus* and samples. The positive control tube contained the culture media and *S. aureus* (in  $5 \times 10^6$  CFU/ml). Other test tubes included culture media with the pathogenic strain (in  $5 \times 10^6$  CFU/ml) and tested compounds at the desired concentration. After 48 h of incubation at 37 °C, the test tubes were examined for possible bacterial turbidity.

### Statistical analysis

Each experiment was repeated three times and the values were reported as the mean  $\pm$  standard deviation. The data were analyzed by SPSS software (SPSS, Inc.,

Chicago, IL, version 20), and  $P < 0.05$  was considered statistically significant.

## RESULTS AND DISCUSSION

### Particle size and zeta potential measurements

The particle size and zeta potential of the four samples prepared in this work are listed in Table I. The particle size of Van/MMT NPs ranged from 270.8 to 572.00 nm. It was found that the particle size of the formulations with a pH of 6 was smaller than those with a pH of 7 at the same temperature. At the same pH, the particle size of the formulations prepared at 50 °C was smaller than those prepared at 40 °C. Moreover, the formulation prepared at a pH of 6 and at 50 °C had the smallest particle size among the others ( $p < 0.05$ ). It is clear that smaller NPs can deeply penetrate into the wound area than the large ones due to their closer contact with the wound bed (Ashtikar, Wacker, 2018).

The zeta potential gives an insight into the stability of NPs in the formulation. A high value of zeta potential (negative or positive) increases the electrostatic repulsion between NPs and prevents their aggregation (Zhao *et al.*, 2019). As shown in Table I, all the prepared formulations exhibited high negative zeta potential values ( $> -30$  mv), suggesting that Van/MMT NPs can form a stable suspension in an aqueous solution. In addition, there was no significant difference between the zeta potential of all prepared formulations ( $p > 0.05$ ), suggesting that pH and temperature conditions did not have significant effects on the zeta potential of Van/MMT NPs.

**TABLE I** - Physical properties of Van/MMT nanoparticles (n=3)

Formulation	Particle size (nm) $\pm$ SD	Zeta potential (mv) $\pm$ SD	Entrapment efficiency (%) $\pm$ SD	Loading efficiency (%) $\pm$ SD
pH 6, T=40°C	460.90 $\pm$ 39.95	- 36.00 $\pm$ 4.35	99.10 $\pm$ 1.16	39.64 $\pm$ 0.46
pH 7, T=40°C	572.00 $\pm$ 33.09	-34.40 $\pm$ 4.25	96.34 $\pm$ 1.36	38.53 $\pm$ 0.55
pH 6, T=50°C	270.8 $\pm$ 77.35*	-35.96 $\pm$ 2.73	100.76 $\pm$ 0.72	40.30 $\pm$ 0.28
pH 7, T=50°C	504.95 $\pm$ 79.95	-35.93 $\pm$ 3.43	98.12 $\pm$ 1.58	39.24 $\pm$ 0.63

Values are expressed as mean  $\pm$  standard deviation followed by the one-way ANOVA test and Tukey's post hoc test with 95% confidence. Montmorillonite (MMT), vancomycin (Van). \*represents a significant difference with other formulations.

## Drug loading percentage

The negative surface charge of the MMT particles allows positively charged molecules to adhere electrostatically to them. In addition, MMT particles possess good cation exchange capacity (CEC) and layer expansion ability that increase their drug loading capacity (Meng *et al.*, 2009; Dening *et al.*, 2016). As seen in Table I, all formulations showed an EE of more than 96% and LEs were around 39%. In addition, different pH and temperature conditions had no distinct influence on the EE and LE of Van/MMT NPs ( $P > 0.05$ ). The high drug loading capacity of all the prepared formulations in the current study could be attributed to the high negative zeta potential values of MMT NPs that could increase their affinity to positively charged Van molecules. The results of the drug loading experiment in the current study are in agreement with earlier studies in which the high zeta potential value of MMT particles increases their drug loading capacity (Kumar *et al.*, 2020). The formulation prepared at a pH of 6 at 50 °C was chosen as the optimum formulation for further studies because its particle size was significantly smaller than the other formulations ( $p < 0.05$ ).

## In vitro release of Van from Van/MMT NPs

The release profile of Van from Van/MMT NPs, prepared at a pH of 6 at 50 °C (Figure. 1), indicates that more than 90% of the drug was released in 360 min ( $95.06 \pm 11.09\%$ ). After 480 min, approximately  $101.96 \pm 11.82\%$  of Van was released from Van/MMT NPs. As

seen in Table II, the  $DE_{360}\%$  (dissolution efficiency at 6 h) of Van/MMT NPs was  $51.02 \pm 11.39$ . MDT for the release of Van/MMT NPs was  $239.87 \pm 19.09$  min. Zhao *et al.* (2019) successfully encapsulated betaxolol hydrochloride (BH) intercalated MMT into the Eudragit®PO (MMT-BH NPs) through the emulsification-solvent evaporation method for the ophthalmic delivery of betaxolol. The EE and drug-loading percentage of their NPs were  $77 \pm 1\%$  and  $8 \pm 2\%$ , respectively. About 80% of betaxolol was released after 10 h (Zhao *et al.*, 2019). Furthermore, another study proved that docetaxel-loaded PLA-TPGS/MMT NPs could increase the half-life of docetaxel greater than 26 times and improved the oral bioavailability of docetaxel from 3.59% for Taxotere® to 78% for the PLA-TPGS/MMT NPs (Feng *et al.*, 2009).

In our study, Van was loaded in MMT to acquire a sustained release behavior of the drug. The release profile of Van from Van/MMT NP in water at 37 °C over 480 min exerted a four-phase release pattern as shown in Figure 1. In the first phase, the drug profile release exhibited an initial release of Van (about  $19.99 \pm 5.74$ ) within the first 120 min, which can be attributed to the Van placed on or near the surface of MMT. In the second phase, the release of the drug can be attributed to the diffusion of drug molecules through the water-filled channels of MMT. Van molecules that are surrounded by MMT layers are released in the third phase, and the last phase is accounted for the gradual interlamellar opening of MMT.

Many mechanisms, such as cation exchange, surface precipitation, adsorption, etc., have been announced to explain the controlled release of drug molecules from MMT (Zhao *et al.*, 2019).

**TABLE II** - The drug release of Van/MMT NP, DE%, and MDT (n=3)

Formulation	Time (h)	% Drug release $\pm$ SD	$DE_{360}\%$ $\pm$ SD	MDT (min) $\pm$ SD
pH 6, T=50°C	6	$95.06 \pm 11.09$	$51.02 \pm 11.39$	$239.87 \pm 19.09$

Values are expressed as mean  $\pm$  standard deviation. Montmorillonite (MMT), vancomycin (Van), nanoparticles (NPs), dissolution efficacy (DE), and mean dissolution time (MDT).

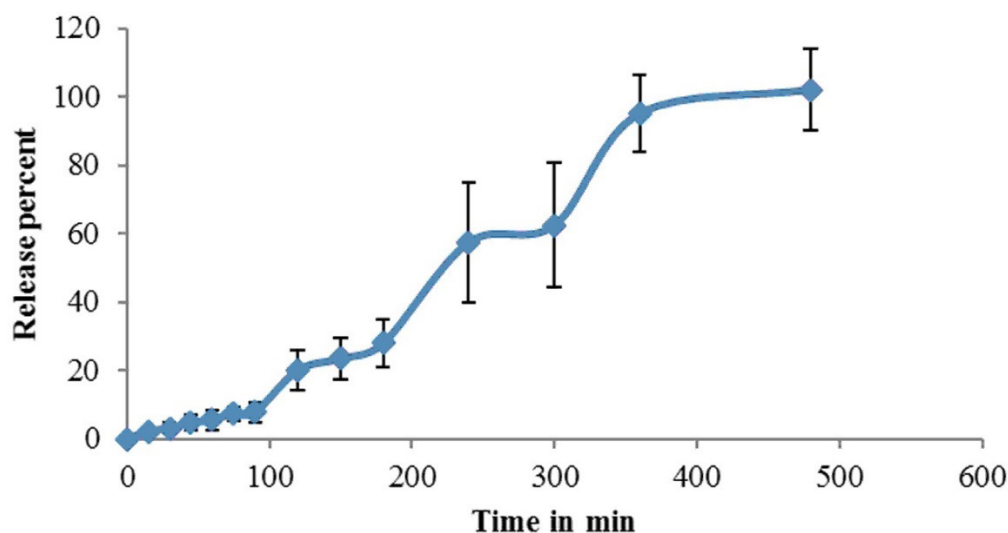


**FIGURE 1** - The *in vitro* cumulative release curve of Van from Van/MMT NPs in deionized water at 37 °C. Van/MMT NPs were prepared at 50 °C and a pH of 6 (n=3). Montmorillonite (MMT), vancomycin (Van), and nanoparticles (NPs).

### ***In vitro* release study of Van/MMT NPs/SA gel**

SA is an anionic linear polysaccharide composed of linear chains of glucuronic (G block), and mannuronic (M block) acid residues. SA is a biodegradable, non-immunogenic, and biocompatible polymer that can transform into the gel that can be used for wound healing applications. Moreover, the cross-linking of alginate chains with cations, such as zinc, can control the release of drugs from the alginate gel (Kurczewska *et al.*, 2015; Tan *et al.*, 2019) particularly foot ulcers. The risk of developing diabetic foot ulcers for diabetic patients is 15% over their lifetime and approximately 85% of limb amputations is caused by non-healing ulcers. Unhealed, gangrenous wounds destroy the structural integrity of the skin, which acts as a protective barrier that prevents the invasion of external noxious agents into the body. Vicenin-2 (VCN-2. Koga *et al.* (2020) swelling profile, mechanical properties, polysaccharide content and X-ray diffraction (XRD) developed a new wound dressing composed of alginate and *Aloe vera* gel, which is cross-linked with zinc ions. The *in vitro* release of Van from Van/MMT NPs/SA gel over time was also evaluated to assess the effect of the SA gel on the release of Van from Van/MMT NPs. The results showed that Van was released in a sustained manner from Van/MMT NPs/SA

gel, and the release rate of Van from Van/MMT NPs/SA gel was slower than that of Van/MMT NPs. As shown in Figure 2, only  $36.18 \pm 7.95$  % of Van was released during the first 7 h of the release study, and  $95.51 \pm 15.39$ % of Van was released over 50 h from Van/MMT NPs/SA gel. Thus, the SA gel could maintain the drug in this structure and exhibit a slower release rate of the drug than Van/MMT NPs. This result is in coincidence with previous studies. For example, Kurczewska *et al.* (2015) prepared Van/halloysite in an alginate base gel. Their results showed that after the placement of Van/halloysite in the alginate base gel, the release of Van was sustained from 70% to 37% after 24 h, indicating the retaining effect of the alginate gel.

Due to the sustained release of Van from Van/MMT NPs/SA gel, the concentration of Van will remain above its MIC and MBC at the infected wound site for at least 24 h and can kill or inhibit microbes, prevent re-infection, and reduce the frequency of secondary complications. In addition, the local sustained delivery of Van can decrease its systemic side effects, protect the wound from infection and contamination, and improve tissue regeneration simultaneously (Kurczewska *et al.*, 2015; Li *et al.*, 2010; Zhang *et al.*, 2017).

Five diffusion models were also fitted to determine the kinetics of drug release for the prepared system. It

is clear from Table III that the release of Van from Van/MMT NPs/SA gel follows Higuchi kinetics, indicating that the release mechanism was governed by diffusion. Furthermore, from the Korsmeyer-Peppas equation,  $n$

is larger than 1, meaning that the release of the drug is categorized in the Super Case II model, which means that the tension and breaking of the polymer occur during the sorption process.

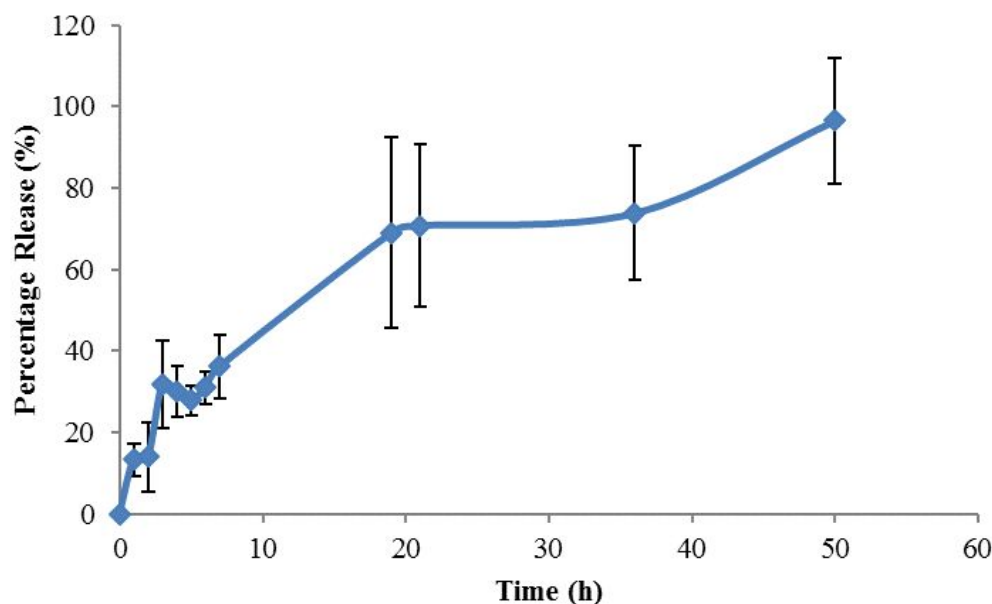


**FIGURE 2** - *In vitro* release of Van from Van/MMT/SA over 50 h at 32 °C in PBS (n=3). Montmorillonite (MMT), vancomycin (Van), and sodium alginate (SA).

**TABLE III** - The fitting results of the *in vitro* release performance of Van/MMT/SA

Release model	Fitting equation	r
Zero-order	$Y = 0.5487X - 10.684$	0.8907
First-order	$Y = -43.576X + 194.36$	0.8537
Hixson-Crowell model	$Y = -17.707X + 78.393$	0.9441
Korse-Meyer peppas	$Y = 1.8162X - 19.869$	0.9409
Higuchi	$Y = 0.0047X + 0.0678$	0.9456

Montmorillonite (MMT), vancomycin (Van), and sodium alginate (SA) gel.

#### Fourier-transform infrared (FTIR) spectroscopy

As seen in Figure 3a, MMT showed characteristic peaks at 3628, 3435, 1199, and 1035  $\text{cm}^{-1}$ , which are attributed to O–H stretching, interlayered O–H stretching, Si–O stretching (out-of-plane), and Si–O stretching (in-plane) vibration for layered silicates,

respectively. Furthermore, peaks at 916, 845, and 795  $\text{cm}^{-1}$  are related to AlAlOH, AlFeOH, and AlMgOH bending vibrations, respectively. The FTIR spectra of Van (Figure 3b) showed the characteristic peaks at 3389, 2934, 2874, 1663, 1588, 1500, 1230, 1062, and 709 belonging to the vibrations of COOH,  $-\text{CH}_2-\text{CH}_3$ , R–NH–R, R–CO–NH<sub>2</sub>, C=O, C=C, phenolic OH, R–O–R, and  $-\text{NH}_2$

stretching, respectively. The main peaks of Van/MMT NP were detected at 3621, 3401, 2934, 2878, 1591, 1673, 1506, 1195, 915, 844, and 795  $\text{cm}^{-1}$ , which are attributed to the O–H stretching, interlayered O–H stretching, –CH<sub>2</sub>–CH<sub>3</sub>, R–NH–R, C=O stretching, –CO–NH<sub>2</sub>, C=C, Si–O stretching (out-of-plane) vibration, AlAlOH, AlFeOH, and AlMgOH bending vibrations, respectively (Figure 3e). Moreover, the characteristic bands of Van and MMT were seen in the physical mixture spectra of Van and MMT (Figure 3d). In the FTIR spectrum of SA powder, the characteristic peaks are evident at 3433, 2924, 1616, 1417, 1090, and 1032  $\text{cm}^{-1}$ , which belong to the O–H stretching, –CH stretching, asymmetric and symmetric stretching of C–O, C–O–C stretching, and C=O stretching, respectively (Figure 3c). FTIR results demonstrated that the original chemical structure of

Van was preserved after incorporation into MMT and in the SA gel. Moreover, almost all characteristic bands belonging to Van and MMT appeared in the spectra of Van/MMT NPs and Van/MMT NPs/SA gel (Figure 3f). Slight shifts of some peaks of Van in the spectrum of Van/MMT NPs can be attributed to the electrostatic interaction between MMT and Van molecules, indicating the successful intercalation of Van into MMT layers following an ion-exchange mechanism, which is in accordance with previous studies (Zheng *et al.*, 2007; Zhao *et al.*, 2019). Moreover, the slight shift in the peaks could be explained by an uneven expansion between MMT layers. The broken adjacent MMT layers could also result in poor crystalline formation, which is responsible for the lower intensity of the peaks in Van/MMT NPs (Zhao *et al.*, 2019).

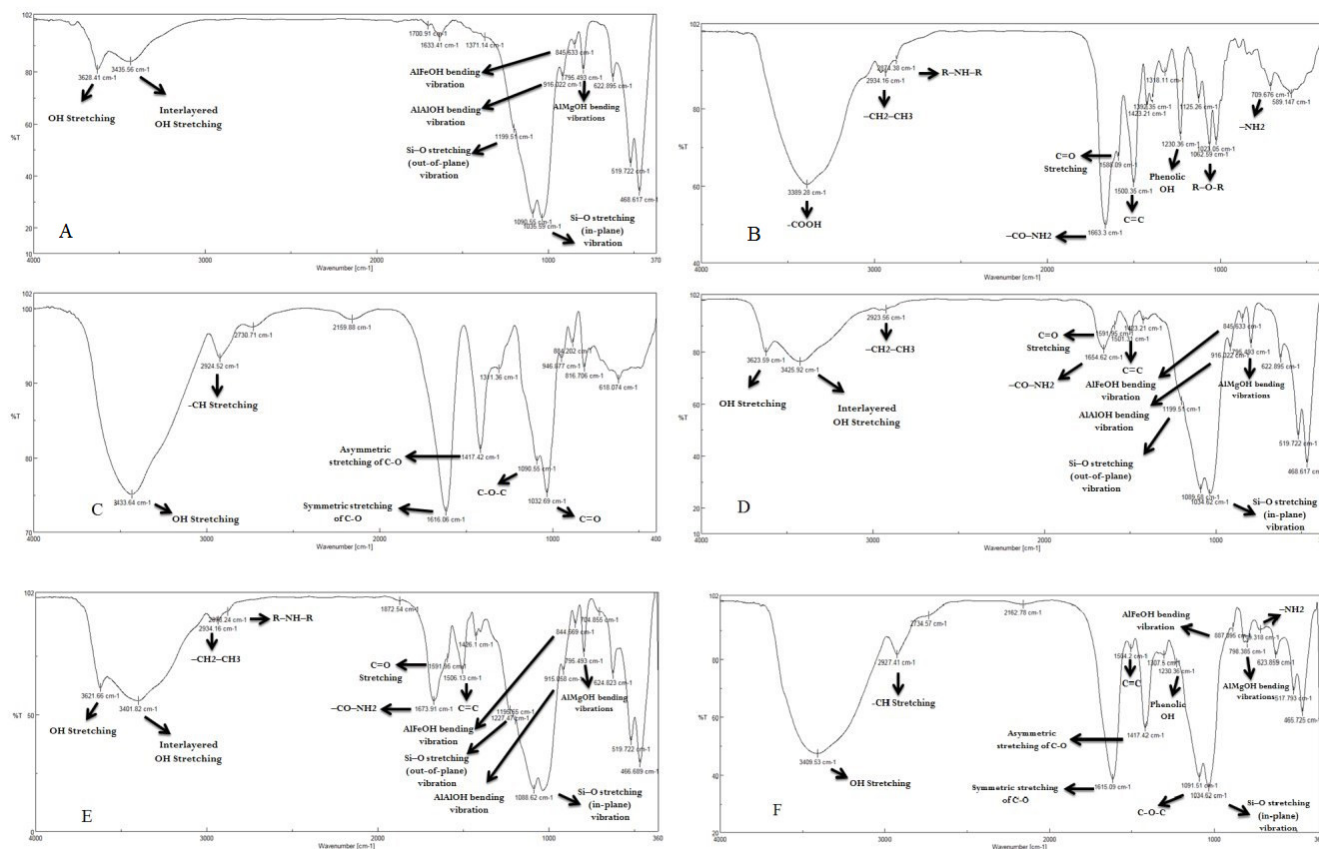


**FIGURE 3** - The FTIR spectroscopy results of a) pure MMT, b) pure Van, c) sodium alginate, d) physical mixture of Van and MMT, e) Van/MMT NP, and f) Van/MMT/SA freeze-dried gel; Montmorillonite (MMT), vancomycin (Van), nanoparticles (NPs), and sodium alginate (SA).

### Morphological studies of dispersions by scanning electron microscopy (SEM)

The SEM images were used to investigate the morphology of MMT and Van/MMT NPs. The SEM images of MMT (Figure 4a) depict the interconnected porous structure of MMT. In addition, MMT showed an irregular shape and nondispersed clay minerals, which might be due to the predominantly alumina (Sabiou *et al.*, 2017). It is proved that no set particle orientation and a multitude of edges, planes, and cavities can be observed in non-dispersed clay, and the particles appear

as aggregated flocs (Sabiou *et al.*, 2017). After loading Van on MMT, the SEM images showed that the smooth surface of the clay turned patchy. Hence, it is confirmed that the drug is highly dispersed on the surface of MMT in the form of nano aggregates (Figure 4b) (Dar *et al.*, 2015).

After Van/MMT NPs were embedded into the SA gel, the final gel was freeze-dried and the SEM image was assessed afterward. As seen in Figure 4c, Van/MMT NPs/SA gel depicts a clear, flat, and wrinkled surface with some macro pores, and the Van/MMT NPs were dispersed uniformly into the gel matrix.

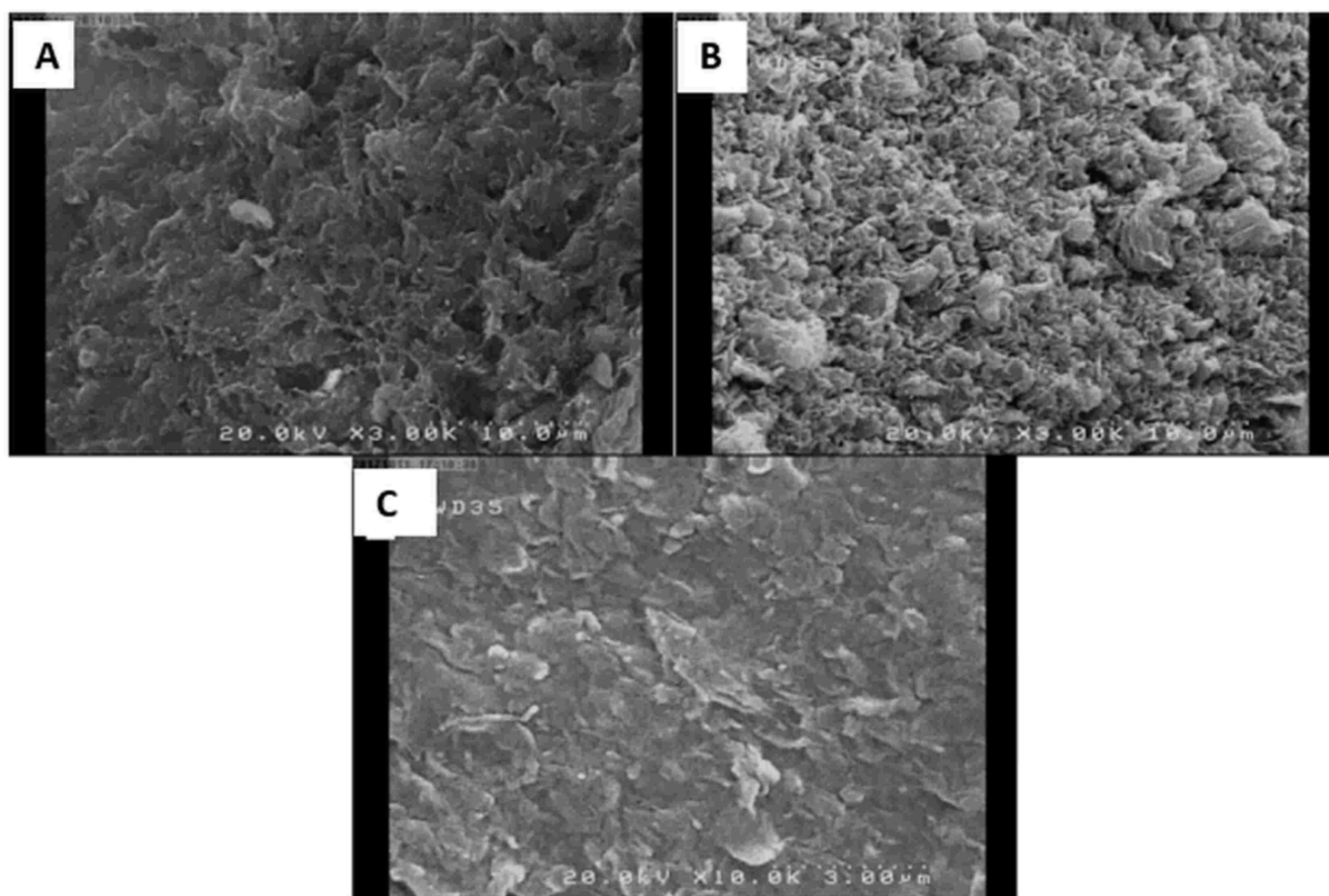


**FIGURE 4** - The SEM micrographs of a) MMT, b) Van/MMT NPs, and c) Van/MMT/SA with a magnification of  $\times 5000$ . Montmorillonite (MMT), vancomycin (Van), nanoparticles (NPs), and sodium alginate (SA).

## Microbial study

The MICs of Van, MMT, MMT NPs/SA gel, Van/MMT NPs, and Van/MMT NPs/SA gel were evaluated against *S. aureus*. The obtained data showed that the MICs of Van, Van/MMT NPs, and Van/MMT NPs/SA gel were  $3.1 \pm 0.4$ ,  $1.4 \pm 0.2$ , and  $0.7 \pm 0.1$ , respectively. A previous study also revealed that the MIC of Van was  $3 \mu\text{g/ml}$  (Booyesen *et al.*, 2019). MMT and MMT/SA gel showed the growth of bacteria in all concentrations indicating that the MICs of these materials are above the studied ranges. Obviously, the MIC of Van/MMT NPs/SA gel was significantly ( $p < 0.05$ ) lower than those of Van and Van/MMT NPs, indicating its promising antimicrobial effect.

The diameters of the zone of inhibition (in mm) in the well diffusion test are shown in Figure 5. The inhibition zone results showed that small inhibition zones were observed for the MMT/SA gel and SA groups, which is in accordance with a previous study (Meng *et al.*, 2009). The inhibition zones of Van, Van/MMT NPs, and Van/MMT NPs/SA gel were significantly greater than those of MMT/SA gel and SA groups ( $p < 0.05$ ). There were no significant differences between the inhibition zones of Van, Van/MMT NPs, and Van/MMT NPs/SA gel ( $p > 0.05$ ). It should be considered that Van/MMT NPs/SA gel was diluted 10 times to be applied in the well diffusion test. Thus, the inhibition zone of Van/MMT NPs/SA gel could be greater than those of Van/MMT NPs and Van without dilution. Thus, the results of the microbial study showed that the loading of Van in MMT (Van/MMT NPs) and the incorporation of Van/MMT NPs in the SA gel could effectively provide the sustained release of Van from the formulation and significantly increase its antimicrobial effect.

Our results are consistent with those of previous studies proving that the incorporation of an antibacterial

agent into MMT could cause the slow release of the drug and improve its antimicrobial effects. For example, Meng *et al.* (2009) prepared chlorhexidine acetate (CA)/MMT intercalation composites and evaluated their antibacterial effects. The CA/MMT showed an initial burst release in 24 h and was then continuously released up to 31% after 72 h. The CA/MMT strongly inhibited the growth of a wide variety of microorganisms, mainly *S. aureus* and *P. aeruginosa*, in which the inhibition zones of CA/MMT against these microorganisms were 24.5 and 21.4 mm, respectively (Meng *et al.*, 2009). The nanocomposite of MMT and chitosan (CS)-loaded silver sulfadiazine (AgSD) was developed in another study. It did not impair cell proliferation but improved the bacteriostatic and bactericidal properties of the drug. While AgSD was microbicide only against *S. pyogenes*, the MMT/CS/AgSD complex showed microbicidal activity 4 times higher than AgSD against *S. pyogenes*, suggesting their good antimicrobial effects at lower concentrations (Sandri *et al.*, 2014) fungi and some viruses. However, AgSD has been shown to be cytotoxic toward fibroblasts and keratinocytes *in vitro* and consequently to retard wound healing *in vivo*. The aim of the present work was to evaluate the *in vitro* biocompatibility (cytotoxicity and proliferation).

The improvement of the antibacterial effect of Van/MMT NPs/SA gel in comparison to Van may be contributed to the small size of Van/MMT NP, which can increase the transport of Van into the wound site and increase the diffusion of the drug into the bacterial cells, possibly reducing both its required dose and side effects. In addition, the sustained releases of Van from Van/MMT NPs/SA gel can retain the concentration of Van above its MIC and MBC at the infected wound site for at least 24 h and can kill or inhibit microbes, prevent re-infection, and reduce the frequency of secondary complications (Rossi *et al.*, 2018; Chen *et al.*, 2012).

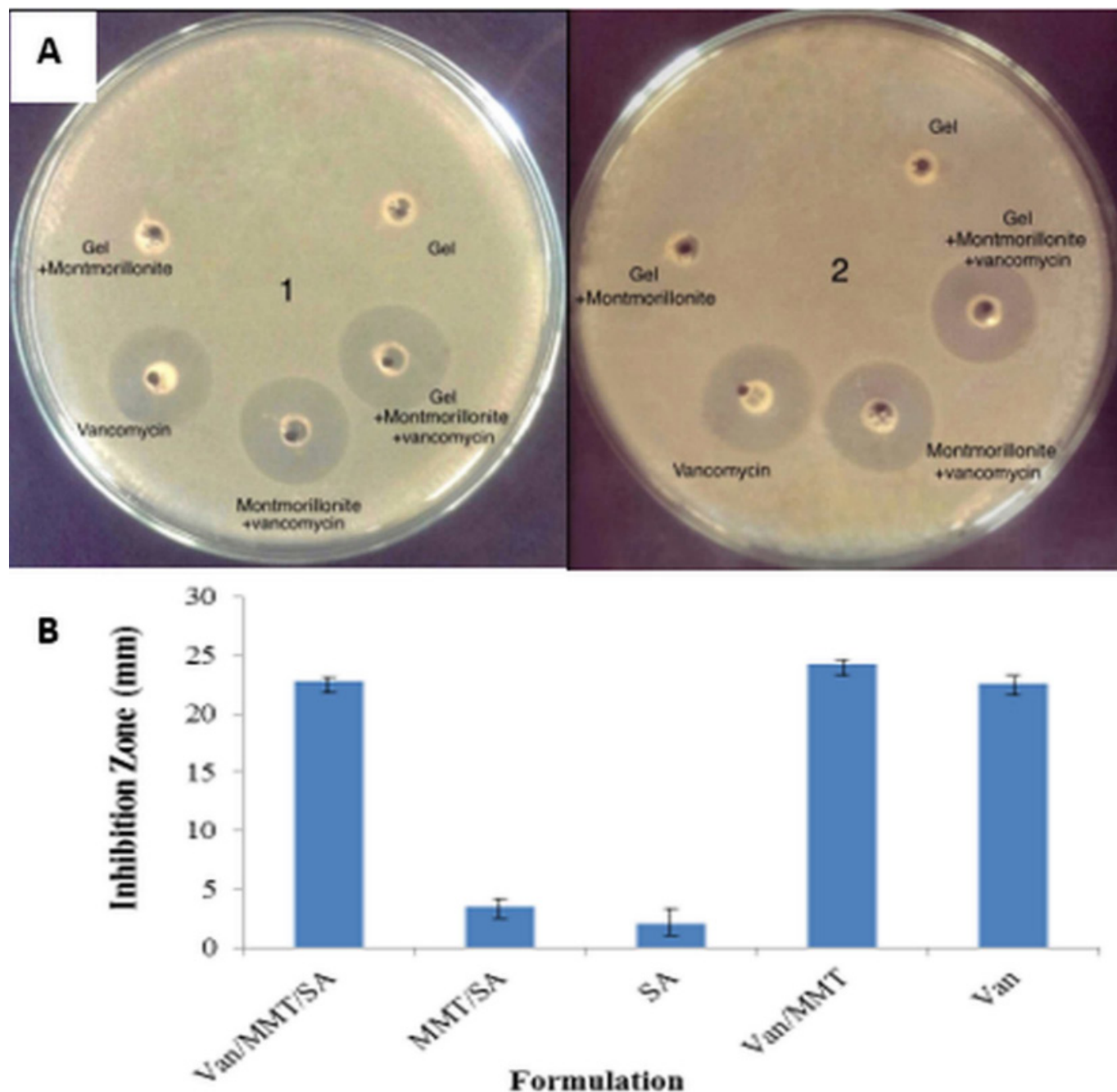


**FIGURE 5** - a) Photographs of the zone of inhibition showing the antibacterial activity for Van, MMT/SA, SA, Van/MMT NP, and Van/MMT/SA against *S. aureus*; b) An enhancement in antibacterial activity against the bacterial strain in terms of the zone of inhibition (mean  $\pm$  SD). Montmorillonite (MMT), vancomycin (Van), nanoparticles (NPs), and sodium alginate (SA).

## CONCLUSION

This study demonstrates that rationally designed Van/MMT NPs/SA gel can be readily prepared with a high drug-loading capacity and a sustained release

pattern of Van. The *in vitro* antimicrobial studies showed that the formulation of an alginate gel-based wound dressing containing Van-loaded MMT NPs (Van/MMT NPs/SA gel) was an efficient method for increasing the antimicrobial efficacy of Van against *S. aureus* for the

treatment of infected wounds. Van/MMT NPs/SA gel can be a promising formulation to treat infected wounds in the clinic.

## REFERENCES

- Ashtikar M, Wacker M. Nanopharmaceuticals for wound healing –Lost in translation? *Adv Drug Delivery Rev.* 2018;129(1):194–218.
- Booyesen E, Bezuidenhout M, van Staden ADP, Dimitrov D, Deane SM, Dicks LMT. Antibacterial activity of vancomycin encapsulated in Poly(DL-lactide-co-glycolide) nanoparticles using electrospraying. *Probiotics Antimicrob Proteins.* 2019;11(1):310–6.
- Chen H-B, Wang Y-Z, Sanchez-Soto M, Schiraldi D. Low flammability, foam-like materials based on ammonium alginate and sodium montmorillonite clay. *Polymer (Guildf).* 2012;53(25):5825–5831.
- Dar B, Pandey N, Singh S, Kumar P, Farooqui M, Singh B. Solvent-free, scalable and expeditious synthesis of benzanilides under microwave irradiation using clay doped with palladium nanoparticles as a recyclable and efficient catalyst. *Green Chem Lett Rev.* 2015;8(2):1–8.
- Dening TJ, Joyce P, Rao S, Thomas N, Prestidge CA. Nanostructured montmorillonite clay for controlling the lipase-mediated digestion of medium chain triglycerides. *ACS Appl Mater Interfaces.* 2016;8(48):32732–42.
- Dong Y, Feng S-S. Poly (d,l-lactide-co-glycolide)/montmorillonite nanoparticles for oral delivery of anticancer drugs. *Biomaterials.* 2005;26(30):6068–76.
- Feng S-S, Mei L, Anitha P, Gan CW, Zhou W. Poly(lactide)–vitamin E derivative/montmorillonite nanoparticle formulations for the oral delivery of Docetaxel. *Biomaterials.* 2009;30(19):3297–306.
- Gelker M, Müller-Goymann CC, Viöl W. Permeabilization of human stratum corneum and full-thickness skin samples by a direct dielectric barrier discharge. *Clin Plasma Med.* 2018;9:34–40.
- Gonzalez AC de O, Costa TF, Andrade Z de A, Medrado ARAP. Wound healing-A literature review. *An Bras Dermatol.* 2016;91(5):614–20.
- Han G, Ceilley R. Chronic wound healing: a review of current management and treatments. *Adv Ther.* 2017;34(3):599–610.
- Hey HWD, Thiam DW, Koh ZSD, Thambiah JS, Kumar N, Lau L-L, et al. Is intraoperative local vancomycin powder the answer to surgical site infections in spine surgery? *Spine (Phila Pa 1976).* 2017;42(4):267–74.
- Joshi G V, Kevadiya BD, Patel HA, Bajaj HC, Jasra R V. Montmorillonite as a drug delivery system: intercalation and *in vitro* release of timolol maleate. *Int J Pharm.* 2009;374(2):53–7.
- Kim H-W, Knowles JC, Kim H-E. Hydroxyapatite porous scaffold engineered with biological polymer hybrid coating for antibiotic Vancomycin release. *J Mater Sci Mater Med [Internet].* 2005;16(3):189–95.
- Koga AY, Felix JC, Silvestre RGM, Lipinski LC, Carletto B, Kawahara FA, et al. Evaluation of wound healing effect of alginate film containing Aloe vera gel and cross-linked with zinc chloride. *Acta Cir Bras.* 2020;35(5):1–11.
- Krzyszczuk P, Schloss R, Palmer A, Berthiaume F. The role of macrophages in acute and chronic wound healing and interventions to promote pro-wound healing phenotypes. *Front Physiol.* 2018;9:419–41.
- Kumar A, Hodnett BK, Hudson S, Davern P. Modification of the zeta potential of montmorillonite to achieve high active pharmaceutical ingredient nanoparticle loading and stabilization with optimum dissolution properties. *Colloids Surf B Biointerfaces.* 2020;193:1–11.
- Kurczewska J, Sawicka P, Ratajczak M, Gajęcka M, Schroeder G. Will the use of double barrier result in sustained release of vancomycin? Optimization of parameters for preparation of a new antibacterial alginate-based modern dressing. *Int J Pharm.* 2015;496(2):526–33.
- Li B, Brown K V, Wenke JC, Guelcher SA. Sustained release of vancomycin from polyurethane scaffolds inhibits infection of bone wounds in a rat femoral segmental defect model. *J Control Release.* 2010;145(3):221–30.
- Masson R, Vuagnat H, Uçkay I, Toutous-Trellu L, Prendki V. Infection of chronic wounds in elderly patients. *Rev Med Suisse.* 2017;13(582):1938–44.
- Meng N, Zhou N-L, Zhang S-Q, Shen J. Controlled release and antibacterial activity chlorhexidine acetate (CA) intercalated in montmorillonite. *Int J Pharm.* 2009;382(1):45–9.
- Menke NB, Ward KR, Witten TM, Bonchev DG, Diegelmann RF. Impaired wound healing. *Clin Dermatol.* 2007;25(1):19–25.
- Norrish K. The swelling of montmorillonite. *Discuss Faraday Soc.* 1954;18:120–34.
- Rebitski EP, Aranda P, Darder M, Carraro R, Ruiz-Hitzky E. Intercalation of metformin into montmorillonite. *Dalton Trans.* 2018;47(9):3185–92.
- Rossi S, Mori M, Vigani B, Bonferoni MC, Sandri G, Riva F, et al. A novel dressing for the combined delivery of platelet lysate and vancomycin hydrochloride to chronic skin ulcers: Hyaluronic acid particles in alginate matrices. *Eur J Pharm Sci.* 2018;118:87–95.

Sabiu B, Mohammed-Dabo IA, Dewu B, Momoh OR, Hamisu A, Abubakar Zaria U, et al. Determination of morphological features and molecular interactions of Nigerian bentonitic clays using Scanning Electron Microscope (SEM). *Bayero J Pure Appl Sci.* 2017;22(9):279.

Salcedo I, Aguzzi C, Sandri G, Bonferoni MC, Mori M, Cerezo P, et al. In vitro biocompatibility and mucoadhesion of montmorillonite chitosan nanocomposite: A new drug delivery. *Appl Clay Sci.* 2012;55:131–7.

Sandri G, Bonferoni MC, Ferrari F, Rossi S, Aguzzi C, Mori M, et al. Montmorillonite–chitosan–silver sulfadiazine nanocomposites for topical treatment of chronic skin lesions: In vitro biocompatibility, antibacterial efficacy and gap closure cell motility properties. *Carbohydr Polym.* 2014;102:970–7.

Schweizer ML, Chiang H-Y, Septimus E, Moody J, Braun B, Hafner J, et al. Association of a bundled intervention with surgical site infections among patients undergoing cardiac, hip, or knee surgery. *JAMA.* 2015;313(21):2162–71.

Stacey M. Combined topical growth factor and protease inhibitor in chronic wound healing: Protocol for a randomized controlled proof-of-concept study. *JMIR Res Protoc.* 2018;7(4):97-108.

Tan WS, Arulselvan P, Ng S-F, Mat Taib CN, Sarian MN, Fakurazi S. Improvement of diabetic wound healing by topical application of Vicenin-2 hydrocolloid film on Sprague Dawley rats. *BMC Complementary Altern Med.* 2019;19(1):20.

Tønnesen HH, Karlsen J. Alginate in drug delivery systems. *Drug Dev Ind Pharm.* 2002;28(6):621–30.

Wang X, Du Y, Luo J. Biopolymer/montmorillonite nanocomposite: preparation, drug-controlled release property and cytotoxicity. *Nanotechnology.* 2008;19(6):1-8.

Wu Q, Li Z, Hong H. Adsorption of the quinolone antibiotic nalidixic acid onto montmorillonite and kaolinite. *Appl Clay Sci.* 2013;74:66–73.

Zhao Y, Li J, Han X, Tao Q, Liu S, Jiang G, et al. Dual controlled release effect of montmorillonite loaded polymer nanoparticles for ophthalmic drug delivery. *Appl Clay Sci.* 2019;180:105-113.

Zhang Y, Liang RJ, Xu JJ, Shen LF, Gao JQ, Wang XP, et al. Efficient induction of antimicrobial activity with vancomycin nanoparticle-loaded poly (trimethylene carbonate) localized drug delivery system. *Int J Nanomed.* 2017;12:1201.

Zheng JP, Luan L, Wang HY, Xi LF, Yao KD. Study on ibuprofen/montmorillonite intercalation composites as drug release system. *Appl Clay Sci.* 2007;36(4):297–301.

Received for publication on 05<sup>th</sup> February 2021  
Accepted for publication on 23<sup>rd</sup> November 2021